Discrete fracture network based drift stability at the Éléonore mine

Grenon M & Landry A
Faculté des sciences et de génie, Département de génie des mines, de la métallurgie et des matériaux, Université Laval, Québec, Canada

Hadjigeorgiou J
Pierre Lassonde Chair in Mining Engineering, University of Toronto, Toronto, Ontario, Canada

Lajoie PL
Goldcorp Éléonore mine, Rouyn-Noranda, Québec, Canada

ABSTRACT

Photogrammetry tools were used to characterise the rock mass structural regime at selected mining drifts at the Éléonore underground mine in Canada. This information was used to provide the input data for generating a series of discrete fracture networks (DFN) models. The generated DFN models were subsequently used to investigate the creation of rock wedges along the drifts that may impact the stability of the excavations. The impact of the choice of employed DFN model on the analysis was investigated with reference to the stability of excavations. A series of parametric analyses demonstrated the sensitivity of the model to variations in the properties of the structural regime. The benefits of using stochastic modelling to capture the inherent variability are reviewed.

1   INTRODUCTION

Over the last decade, the use of DFN became widespread, partly because of recognition of their potential, and improved computer performance. Initially applied in hydrogeological and petroleum engineering applications, DFN are now an integral part of scoping studies and engineering design for several civil and mining projects, (Elmo et al. 2014; Grenon and Hadjigeorgiou 2003a, 2003b, 2008b, 2012; Rogers et al. 2006, 2009, 2015). Nevertheless, DFN are rarely used in the design of mining drifts.

DFN modelling relies heavily on the quality of the input structural properties data gathered in the field. Traditionally, joint sampling methods rely on manual mapping of the rock face using scan lines or scan windows (Hadjigeorgiou et al. 1995; Kulatilake and Wu 1984; Pahl 1981; Priest and Hudson 1976; Zhang and Einstein 1998). Manual scanning methods are time-consuming and thus often not used in an operating environment such as a mine in production. The result is a relative absence of comprehensive field data that can be used for stability analysis of excavations in rock.

Digital mapping techniques, based on the acquisition of point clouds on the rock surface through terrestrial laser scanning (TLS) or photogrammetry, have been gaining popularity in recent years. Following the data collection, the fractures' geometrical properties are analysed using computer tools. Several authors discuss the merits and limitations of these mapping techniques (Birch 2006; Dubois and Grenon 2012; Gaich et al. 2006, 2008; Grenon et al. 2004; Haneberg 2008; Kemeny et al. 2006; Sturzenegger and Stead 2009; Sturzenegger et al. 2009).

This paper presents a case study at the Éléonore project, an underground hard rock mine in Eastern Canada where photogrammetry data were used to provide the input parameters to generate a series of DFN models. The generated models were employed to investigate the stability of drift. The influence of the choice of DFN model on the analysis was explored. Furthermore, the model sensitivity to the variability in the properties defining the structural regime was also addressed.

2   ÉLÉONORE PROJECT

The Éléonore project is located in the James Bay region, on the shore of the Caniapiscau Reservoir, Fig. 1. It is one of the most important gold-bearing mining projects in development in Canada. Production began during the last quarter of 2014 and is scheduled to reach 7000 t/day.

The operation utilises a ramp access from the surface and two shafts 725 and 1500 m in depth. The orebody is sub-vertical, and is exploited using the long-hole mining method. Mining is planned to take place in two phases, the first one between the depths of 80 and 650 m, and the second phase between 650 and 1400 m (Lajoie 2013). The Éléonore project is highly mechanised, and the hauling drifts and the draw points have a typical cross section of 5.5 × 5.5 m.

From a geological perspective, the Éléonore property is centred on the Ell Lake intrusion (a small diorite stock bordering the batholithic complex), and straddles the contact between the Opinaca metasedimentary sub-province and the La Grande volcano-plutonic sub-province.

The most common unit is metasomatised greywacke (more than 11 possible declinations), which is fine-grained and usually medium grey with a quartzofeldspathic matrix. Other major geological units include diorite, diabase, arenite, conglomerates and pegmatite dikes at a scale varying from small centimetric veins to metric dykes. The host rock in the mineralised zones is usually a thinly bedded greywacke (SRK Consulting 2011).

A strong presence of sub-horizontal fractures was observed from the surface down to 400 m below the ground. At greater depth, the intensity of this fracture set is less pronounced although it is still observed regularly. Sub-vertical fracture sets with various orientations were also observed at Éléonore (Golder Associates 2008).

Figure 1. Goldcorp Éléonore project location © Gouvernement du Québec

3 STRUCTURAL DATA COLLECTION AND ANALYSIS

A major challenge in an operating mine is collecting the necessary field date to characterise the rock mass. At Éléonore, the geomechanical data collection process made use of a commercially available 3DM analysis mapping suite (v 2.5.0) from ADAM Technology (2010). Digital images were taken during development of three rock faces and were used to construct a 3D numerical model of the rock mass in three mining drifts, Amn-0354, Gmn-0354-1s and Gmn-0357-1n. The drifts were at the 440 level within a radius of 50 m and at less than 10 m from the mineralisation, Fig. 2. The general face orientation was 88°/252°, 87°/185° and 86°/161° for the Amn-0354, Gmn-0354-1s and Gmn-0357-1n drifts, respectively. The lithology was mostly composed of lightly metasomatised greywacke. A two-man crew took two hours to complete the field work at each face. This included the digital rock mass scanning and surveying.
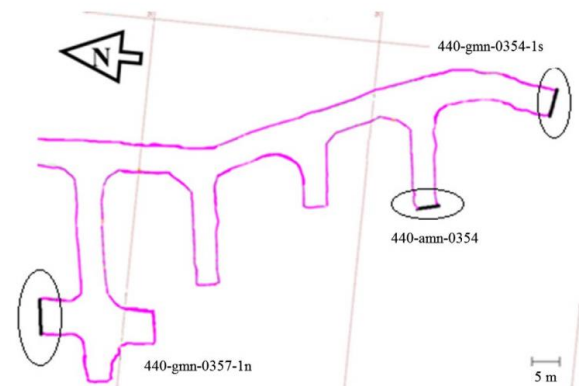

Figure 2. Location of the three development rock faces

Twelve digital images were recorded in every drift. The 3D numerical models of the fractured rock mass were constructed using these photographs. The 3DM analyst was used to match similar points between the various pictures. A digital terrain model (DTM) was created for every drift. A synthetic surface was created from the DTM and the digital images were superimposed on the surface. It took less than two hours of processing, including file transfer and management, to construct the DTM for each drift. Figure 3 presents the DTM with superimposed pictures for two drifts.

The main geometrical components recorded through structural mapping are orientation, spacing, size and intensity of fractures (Dershowitz and Einstein 1988). Digital or 'virtual' structural mapping was conducted on the DTM using the 3DM Analyst. The fracture traces were visually identified on the images. Points were selected on the identified traces. The orientation of the fracture planes was computed within the 3DM Analyst and represented by a 3D circle on the rock face. The results are presented in Fig. 3. All fractures are defined by their centre coordinates, trace lengths and orientation.

All identified fractures in the 3DM Analyst were exported to Dips (Rocscience 2011). In all, four dominant

joint sets were identified from the stereonet plots. The mean orientations were determined for each joint set and the dispersion around the mean orientation values was quantified using the Fisher distribution. Figure 4 presents the stereonet plot for all sampled fractures on level 440.

Trace length sampling is susceptible to four major biases (Zhang and Einstein 1998): orientation bias, size bias, truncation bias and censoring bias. In this investigation, fracture trace lengths were determined from the constructed models using the sampling approach proposed by Zhang and Einstein (1998). This approach minimises bias and allows for a non-biased estimation of trace lengths for all joint sets. The nonbiased trace length estimator μ was calculated using Equation 1.
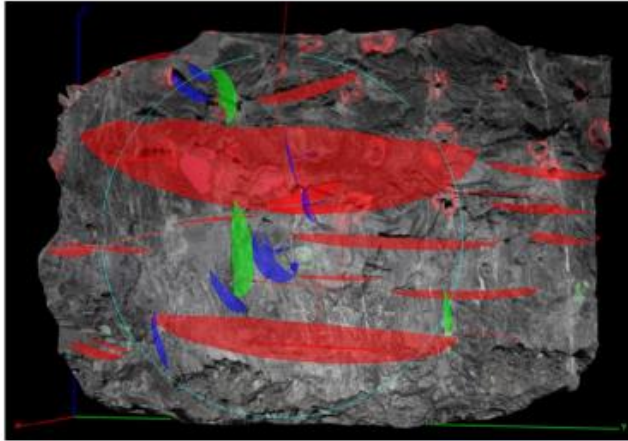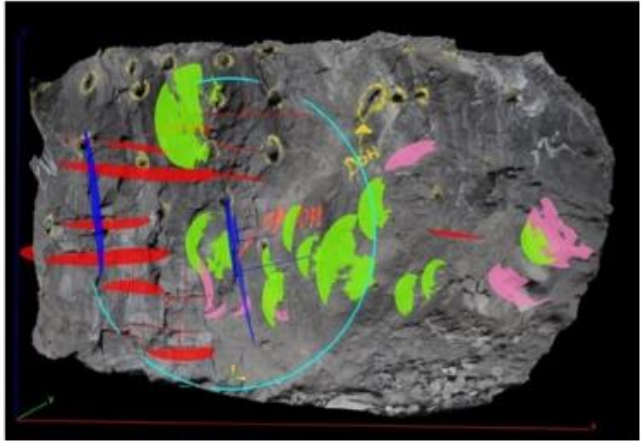

Figure 3. a Amn-0354 3D face model with major discontinuity sets mapped using a 2-m-raidus mapping window; b Gmn-0357-1n 3D face model with major discontinuity sets mapped using a 2-m-radius mapping window
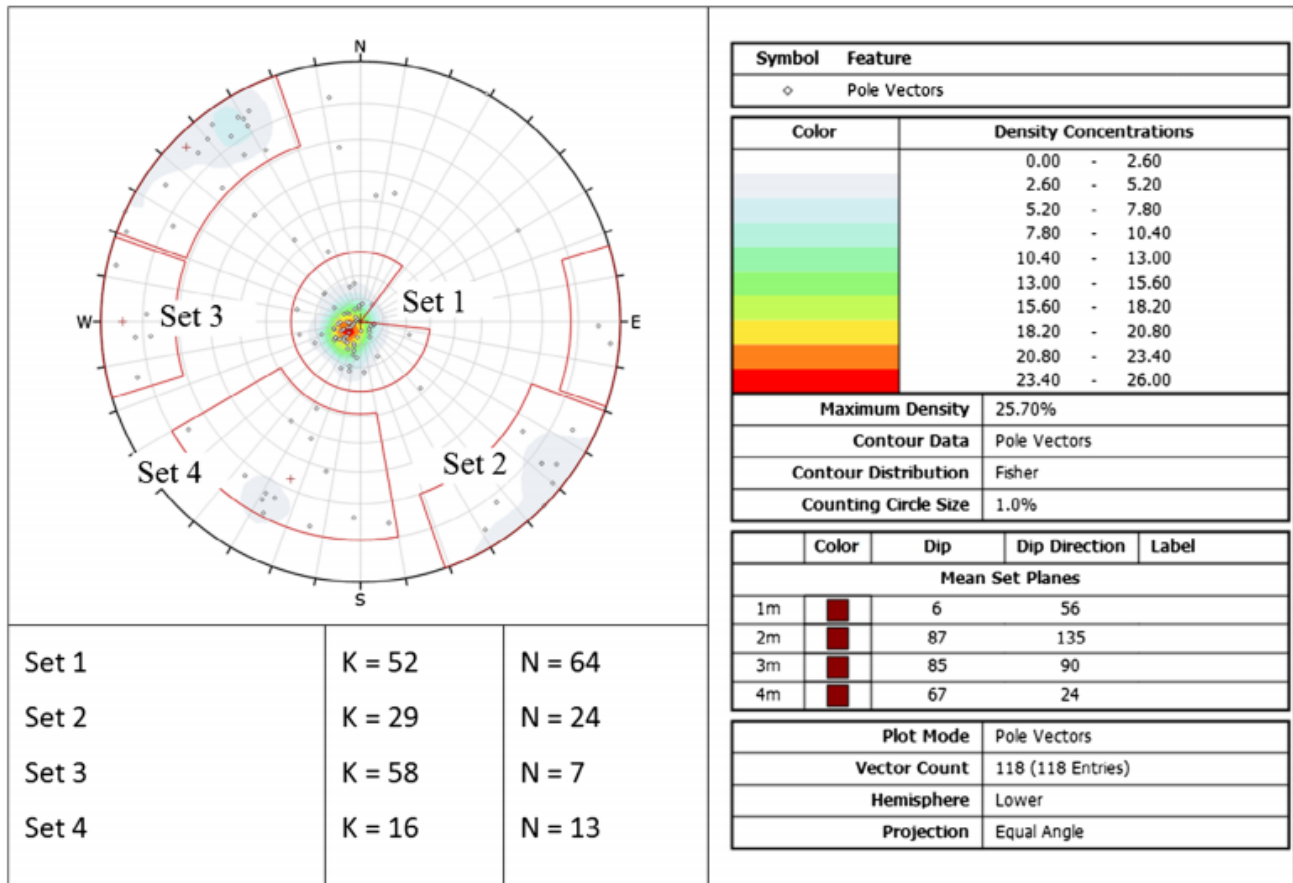

Set 1	K = 52	N = 64
Set 2	K = 29	N = 24
Set 3	K = 58	N = 7
Set 4	K = 16	N = 13

Symbol	Feature
◇	Pole Vectors

Color	Density Concentrations
	0.00 - 2.60
	2.60 - 5.20
	5.20 - 7.80
	7.80 - 10.40
	10.40 - 13.00
	13.00 - 15.60
	15.60 - 18.20
	18.20 - 20.80
	20.80 - 23.40
	23.40 - 26.00

Maximum Density	25.70%
Contour Data	Pole Vectors
Contour Distribution	Fisher
Counting Circle Size	1.0%

	Color	Dip	Dip Direction	Label
		Mean Set Planes		
1m		6	56	
2m		87	135	
3m		85	90	
4m		67	24	

Plot Mode	Pole Vectors
Vector Count	118 (118 Entries)
Hemisphere	Lower
Projection	Equal Angle

Figure 4. Stereonet of mapped fractures

$$\mu = C \frac{\pi\,(N + N_0 - N_2)}{2\,(N - N_0 + N_2)} \qquad\qquad [1]$$

where:

C = Radius of the circular sampling window.

N = Total number of traces intercepting the window.

N_0 = Number of traces with two extremities contained within the sampling window.

N_2 = Number of traces with two extremities lying outside of the sampling window.

In the Éléonore case study, the mapping window radius was selected to maximise its size at the rock face. The maximum traces sampled on the faces were also evaluated. Random fractures were ignored due to their low occurrence (less than 5% of the mapped fractures). Fracture trace length was relatively small with a mean value around 1 m or less. This would classify these joint sets as low to very low persistence based on Brady and Brown (2004). The histograms of fracture traces for every set are presented in Fig. 5. Based on Kolmogorov–Smirnov (KS) test results (α = 5%), a lognormal distribution was judged most appropriate for the trace lengths.

Fracture intensity can be calculated by several qualitative and quantitative techniques. In this paper, in order to maximise the surface information available from the digital images, fracture intensity was calculated for every joint set based on the summation of trace lengths per unit area (P21), as defined by Mauldon and Dershowitz (2000). The fracture intensity for joint set 1 was considerably higher than those of the other three joint sets.

The fracture properties obtained through the photogrammetry campaign at Éléonore are presented in Table 1. These structural properties were deemed adequate to represent the metasomatised greywacke on level 440 at the mine. The use of photogrammetry expedited the data collection process in an operating mine and provided the input data for the subsequent analysis.
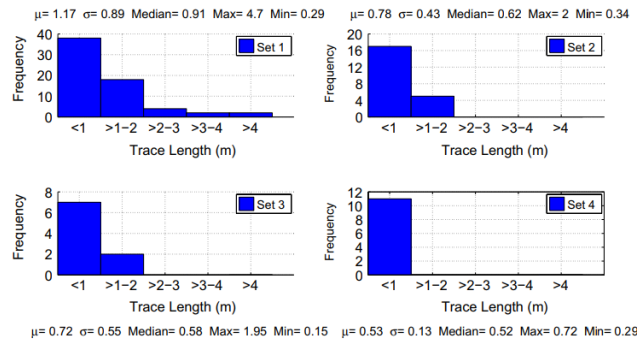

Figure 5. Histograms of the fracture sets' trace length distributions

4 DFN MODELLING

Staub et al. (2002) provided an excellent review of models that can be used to generate DFN. The majority of DFN generation models have been implemented in proprietary or commercially available software packages. For generating fracture system models, for the Éléonore project, the authors employed a software package, Fracture-SG, Grenon and Hadjigeorgiou (2008).

The forward modelling technique was used to calibrate the generated fracture systems. The methodology used by the authors has been presented in several publications (Esmaeili et al. 2010; Grenon and Hadjigeorgiou 2003a, 2003b, 2008; Hadjigeorgiou et al. 2009). In this case study, several DFN generations were necessary in order to achieve statistical agreement between the modelling results and the field data obtained using photogrammetry. Scan planes were introduced in the DFN and the fracture properties on these planes were compared to photogrammetry results. A typical calibrated DFN with a volume of 20 × 20 × 20 m had more than 18,000 fractures. To validate the DFN models, scan planes with the same orientation as the underground rock faces were simulated through the models. The intercepted fractures along these scan planes were calibrated until a good agreement was observed for mean orientation and dispersion for every set. Fractures were subsequently calibrated to their mean trace lengths. Seven scan planes were introduced within every model, each containing five randomly located circular sampling windows, with a radius equal to the radius for the photogrammetry analysis, to sample the fractures.

The DFN models were adjusted until a satisfactory statistical agreement was achieved between field and model data. Fracture intensities (P21: total trace length of fractures per unit area) were then calibrated until satisfactory agreement was reached. Among other tests, the Kolmogorov–Smirnov test was used to compare orientation and trace length statistical distributions of the in situ and the modelled fracture sets. A 5% significance level was selected to accept or reject the null hypothesis that the field and simulated data belong to the same distribution. This calibration process was repeated until statistical agreement was reached between the field data and simulated data. Subsequently, the validated DFN was accepted as a plausible representation of the in situ fracture system. Since fracture system models are based on stochastic generation, the fracture system used in this particular analysis is only one of many possible systems. The whole calibration process was greatly facilitated by enabling easy direct comparisons between field information, provided by photogrammetry, and generated fractures.

Table 1. Fracture properties based on the photogrammetry campaign

Joint set	1	2	3	4
Mean dip (°)/dip direction (°)	06/056	87/135	80/0090	67/024
Fisher's K constant	52	29	58	16
Unbiased trace length (m)	1.20	0.90	0.46	0.60
Trace length (std)	0.89	0.43	0.55	0.13
Maximum trace (m)	4.70	2.00	1.95	0.70
P_{21}	1.40	0.47	0.21	0.26

5 DETERMINING DRIFT STRUCTURAL STABILITY USING DFN

DFN modelling can be used for several applications in underground mines. The focus of this paper is the identification of structural wedges formed along mining drifts. In the early stages of mining at the Éléonore project, during development of the drifts, the formation of structurally defined wedges was observed on a few occasions. In this context, structurally defined wedge instability along the walls was a concern. A series of DFN models were used to investigate the creation of wedges along the walls and the roof of typical mining drifts at Éléonore.

Once a DFN model was constructed and calibrated, the drift was introduced in the rock mass. The first step of the analysis was to investigate the formation of wedges along a 17-m-long drift. Figure 6 i llustrates the wedges formed along the drift for one specific DFN generated using the Baecher model. This analysis included all generated wedges that had a free face along the mining drift. Structurally defined wedges could be encompassed in larger wedges. Nevertheless, the stability analysis considered each wedge individually. The following sections address fundamental issues concerning the use of DFNs such as the choice of the model, variability in input data and number of simulations to obtain representative results.
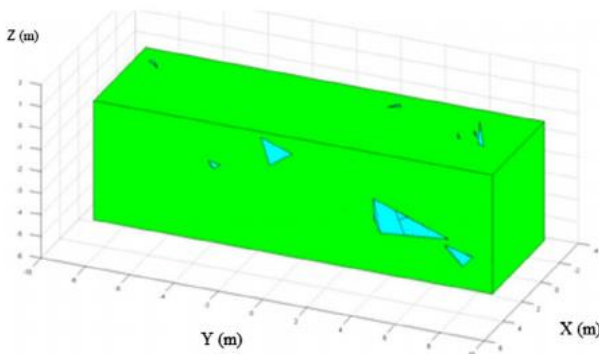

Figure 6. Illustration of wedge generated for he max fracture representation along a 17-m drift

6 SELECTING A DFN MODEL

A discussion that appears to be missing in DFN applications in mining is the impact of the selected model on the engineering analysis. In theory, several DFN models can be used to represent the structural conditions at a given site. Successfully calibrated DFN can provide good statistical agreement with field data and the conclusion is inferred that the models are acceptable. Nevertheless, the various DFN models can have considerably different geometrical characteristics that can have a significant impact on the analysis and interpretation. This was demonstrated in this investigation by employing four different DFN models and the resulting wedges formation along the drift in Fig. 7.

The following models were used in this analysis: Baecher, BART, nearest neighbour and Veneziano. A short summary of these models is reproduced in Sections Baecher model, Enhanced Baecher model, Baecher algorithm, revised terminations (BART) model, Nearest neighbour model, and Veneziano model from the more extensive work of Staub et al. (2002).

6.1 Baecher model

The major feature of the Baecher model is the assumption of circular fracture shape. The following geometric parameters are required to generate the DFN: density of the fractures (number of fractures per unit volume), the orientation distribution of these fractures, the size and shape of the fractures. Fracture centres are located uniformly in space, using a Poisson process and the fractures are generated as discs with a given radius and orientation. As a result of the fracture location, shape and size process of the model, fractures terminate in intact rock and intersect each other. Any combination of fracture size, location and orientation assumptions are possible

6.2 Enhanced Baecher model

The enhanced Baecher model has the same geometric requirements as the Baecher model. In this variation, however, it is possible to account for fracture termination at intersections with pre-existing fractures. The model employs the concept of termination probability, defined as the probability that a fracture of a given set will terminate when it intersects a fracture of an earlier set. The enhanced Baecher model can accommodate more general fracture shapes, defined by polygons.

6.3 Baecher algorithm, revised terminations (BART) model

This model has the capacity to generate non-uniform fracture locations. The basic difference from the enhanced Baecher model is the way it treats fracture termination modes. In the BART model, termination is assigned by termination percentage: the percentage of fractures that terminate at intersections with other fractures. It is suggested that this approach can provide a better correlation to field data than other variations of the Baecher model. As the locations of secondary fractures are controlled by the locations of the primary fractures, in the BART model, the resulting fracture populations exhibit spatial correlation and tend to occur in clusters or chains.

6.4 Nearest neighbor model

The nearest neighbour model is a semi-stochastic, pattern-based model. It differs from the enhanced Baecher model in the way it manages the spatial distribution of fractures. It is capable of simulating fractures clustered around major points and faults by preferentially producing new fractures in the vicinity of earlier fractures. This is achieved in the nearest neighbour model by organising and generating fractures in sequence into primary, secondary and tertiary groups. In this approach, fractures in the primary groups dominate the generation of fractures in succeeding groups.
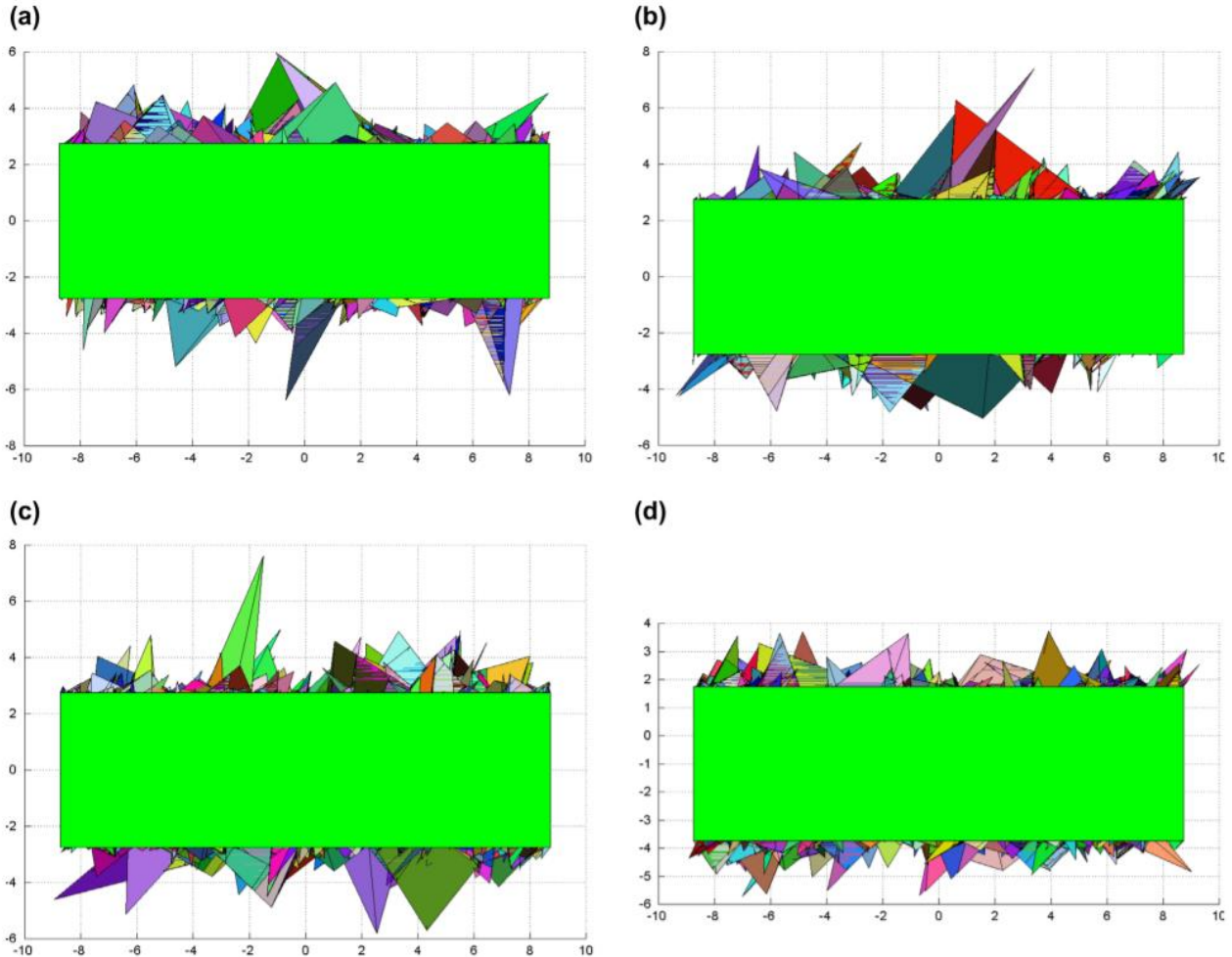
Figure 7. Wedge formation on the walls of a horizontal drift using *a* an Beacher model, *b* a BART model, *c* a nearest neighbour model and *d* a Veneziano model

The probability of a fracture at a point x in three-dimensional space is given by:

$$P_x(x) = CL^{-b} \qquad [2]$$

Where L is the distance from point x to the nearest fracture of a previous, dominant group, and b and C are empirical constants.

The same input data are used as for the enhanced Baecher model with additional data on the spatial interrelationship of the fractures. The nearest neighbour model can also use the termination probability

6.5   Veneziano model

The Veneziano model relies on the generation of a Poisson network of planes in 3D space followed by a secondary process of tessellation by a Poisson line process and marking of polygonal areas. A portion of these polygons is randomly marked as jointed, while the remainder is defined as intact rock. The Veneziano model is similar to the Baecher model with the exception that fractures are represented by coplanar line segments. Use of the

Veneziano model results in an exponential distribution of fracture trace lengths, rather than lognormal distribution as generated in the Baecher model.

6.6   DFN model comparison

This section describes the investigation into the influence of the choice of DFN model on the generation of structural wedges along the 17-m-long drift at Éléonore. Fracture-SG was used to generate DFN using the models described in this section. DFN based on Baecher, BART, nearest neighbour and Veneziano models were generated. All generated models were calibrated using the KS testing procedure and considered representative of the same rock mass conditions. Some features of the various models, rarely discussed in the literature from a validation point of view, such as joint terminations, set hierarchy or coplanarity were added to the various DFN. These features were not meant to specifically represent field conditions at Éléonore, they were added to see the potential impact on the wedge formation results since they are rarely addressed in the validation process. These additional

features contribute to the intrinsic characteristics of the various models.

The DFN based on the Baecher model considered fracture termination in intact rock. The BART model was generated considering that sets 2, 3 and 4 had a 100% termination on set 1, thus creating systematically connecting fractures. The nearest neighbour model generated considered that set 1 was the primary set, while the three other sets were secondary to set 1, thus creating clusters of fractures around fractures of set 1. In this case, generated fractures terminated in intact rock and a "b" value of 2 and a "C" value of 1 were assigned to the three fracture sets. The Veneziano model intrinsically considers coplanar fractures.

The validation procedure employed in this analysis, for all fracture sets for all models (Baecher, Enhanced Baecher, BART, NNM), is illustrated with reference to fracture set 1 of the Baecher model. The same procedure was used for all fracture sets and models.

Seven sampling scan planes were introduced within the simulation volume. The sampling scan planes had the same orientation as the rock exposures mapped in the field. Hundred circle sampling windows were randomly assigned on every scan plane. These windows were used to collect the structural data used in the calibration process.

The mean orientation of fracture set 1, based on the field data, was 06o /056 o and a K factor of 52, Table 1. The DFNBaecher-generated data for fracture set 1 were defined by a mean orientation of 06°/056° and a K of 53. These values are consistent with the field data. Based on the methodology proposed by Fisher et al. (1993), the mean value and dispersion modelled were compared with field data. A student hypothesis test (α 5%) was used to compare the mean orientation resulting in a p value of 0.99. Consequently, it was not possible to reject the null hypothesis that the two values are statistically equal. A Fisher hypothesis test (α 5%) was performed to compare the dispersion around the mean value resulting in a p value of 0.40. This did not allow the rejection of the null hypothesis.

The trace length data were analysed using the approach proposed by Zhang and Einstein (1998). The unbiased mean trace length was 1.20 m. The distribution of the traces intercepted by the sampling window showed a standard deviation of 0.89 and was best represented by a lognormal distribution. The unbiased mean trace length was evaluated based on 100 sampling windows. A value of 1.21 m was obtained. This is comparable to the field value. For the fractures that were intercepting the sampling windows within the DFN-Baecher, traces were obtained. Using a KS test for two samples, the distributive natures of the modelled and field data were compared. A p-value of 0.82 was obtained, thus it was not possible to reject the null hypothesis that these two samples are statistically similarly distributed.

Field data for P21 are indicating a value of 1.40. The average P21 value obtained on the 100 sampling windows is giving a value of 1.39. Again this is comparable to the field value. On the 100 sampling windows, the STD obtained for P21 is 0.33 that suggests some variability in the results. This comprehensive and rigorous approach was used to calibrate the fracture set properties for all sets for all the DFN models used in the paper.

Given that some geometrical characteristics of the four models are dissimilar, the number of generated wedges along the excavated drift excavated in these DFN rock masses could be different. This is demonstrated in Fig. 7 showing the volume of wedges along the walls of a horizontal drift at Éléonore.

The graphs in Fig. 8 are scatter plots of all wedges formed along the walls of the drifts. This series of graphs serves to illustrate the resulting wedges along the drift, formed as a result of the interaction of the different joint sets. In effect, it identifies the joint sets that define the three faces of a wedge. Following the generation of these wedges, the stability of each wedge was determined using a limit equilibrium analysis. Wedges with a factor of safety > 1 are indicated as stable in Fig. 8.

The practical implications for this particular analysis are that the DFN generated using the Veneziano model, for this drift configuration, resulted in the formation of smaller wedges with none of them exceeding a weight greater than 1 t. The investigation based on the Baecher-generated DFN indicated the generation of considerably larger wedges, both stable and unstable. This was the case for the analysis based on the BART model where joint termination on other joint was maximised. The stability implications on the use of the nearest neighbour model are less critical, even if clustering of joints was modelled.

Even if a limited number of DFN were modelled, this example clearly demonstrates the possible impact of the choice of DFN model on the structural stability of a drift. In this example, use of the Veneziano-generated DFN results in smaller wedges that are less of a concern for stability purposes. The results can be explained by the fact that low P32 values associated with small fracture size may be less prone to creation of wedges locally in Veneziano-based DFN than in the more uniform fracture distribution in the Baecher model. To the author's knowledge, the influence of the DFN model on the results is often overlooked or ignored. For engineering purposes, it is necessary to ensure that the generated DFN model is representative of the geological field conditions. In this particular case study at the Éléonore project, the Baecher model was the most appropriate. In this particular location and ground conditions, field observations did not support the presence of strong joint coplanarity as required by the Veneziano model. Furthermore, there was no evidence of joint termination on other joints as modelled by the BART model nor strong joint clustering as modelled by the nearest neighbour model. The photographs of the rock faces mapped, presented in Fig. 3, further corroborate these observations.

7 WEDGE STABILITY ANALYSIS USING MULITPLE BEACHER-DFN REALISATIONS

Based on the assessment of the four models, the Baecher model was chosen for subsequent investigations. The need for multiple simulations is sometimes overlooked in some of the technical literature. In this particular case study, recognising the stochastic nature of DFN, and in

order to fully capture possible wedge formation, a total of 120 DFN models were generated (almost 2 km of drift). For all cases, two drifts were inserted within every DFN.

The structurally defined rock wedges along the walls and backs of each drift were determined for the 120 generated DFN. The limit equilibrium method used to evaluate the structural stability of underground excavations was presented in detail in Grenon and Hadjigeorgiou (2003b). Several examples are available where this methodology was used to evaluate the stability of wedges in underground mines at the periphery of mining stopes, Grenon and Hadjigeorgiou (2003b), on the walls of mining drift, Grenon and Hadjigeorgiou (2003a), on the walls of ventilation raises (Hadjigeorgiou and Grenon 2005) and the walls of ore passes (Hadjigeorgiou et al. 2009). For all joints sets, it was deemed adequate to use cohesion of 0 and friction angle of 30 as preliminary values based on field observations. These are the design values employed at the mine site.

Table 2 summarises the results for this typical drift. Only a relatively small number of wedges were created

along the drift. Wedge-type instability does not seem to pose a real major concern for these drifts, given the size of the wedges (maximum 0.070 m^3). The inherent assumption of course is that the generated DFN models capture the complexity of the rock mass

Table 2. Wedge properties for 240 drifts within 120 DFNs

	DFN input (Baecher model)
Total number of wedges	1772
Mean no. of wedges per drift	7.8
Maximum volume (m^3)	0.070
Volume 99th percentile (m^3)	0.012
Volume 95th percentile (m^3)	0.0026
Volume 90th percentile (m^3)	0.0010

8 IMPACT OF VARIATIONS IN P_{32} AND TRACE LENGTHS

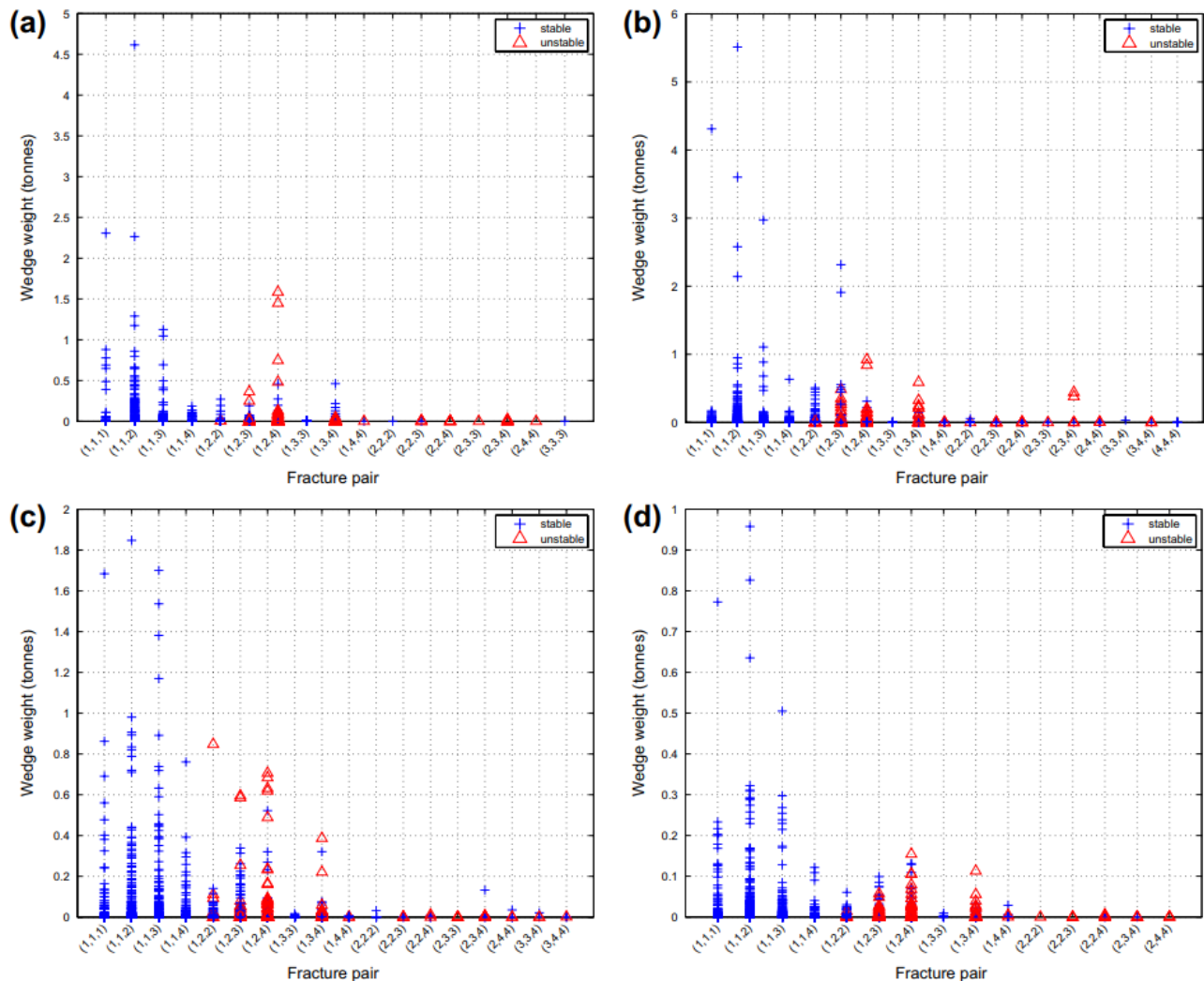In most cases, the input parameters used for a DFN analysis consist of a mean value and its corresponding

Figure 8. Wedge properties on the walls of a horizontal drift using *a* an Beacher model, *b* a BART model, *c* a nearest neighbour model and *d* a Veneziano model

distributions. Recognising that the structural information was obtained from a relatively small sample, which is often the case in mining projects, it was decided to further investigate the impact of variations in the input data on the generation of rock wedges along the excavation.

The objective of this work is to highlight the potential impact of variations of fracture size and/or the fracture intensity on the resulting wedge formation. Three scenarios of input data were investigated in generating DFN using the Baecher model with 120 generations each. The first case used the in situ properties determined from field mapping (mean), the second case employed the maximum trace length for the mean value, but at the same time keeping the P_{32} value constant (max). Finally, the third scenario used the maximum trace length as the mean value and increased P_{32} (worst). The last scenario results in a heavily jointed rock mass. Both the mean and max simulations were based on the same total fracture area over the entire simulated volume (P_{32}). Max and worst simulations employed the same fracture size distributions to generate the DFN. Figure 9 is an example of the generated DFN for joint set 1 using the three approaches (mean, max and worst). The generated DFN were calibrated using KS and statistical tests to compare the simulation results with the target input values associated to the investigated scenarios.

Table 3 summarises the characteristics of all generated rock wedges, along the walls and back of the drift, for the three DFN input scenarios. The mean number of wedges formed along each drift is the average, determined from two drifts, in the 120 DFN simulations. There is a significant variation in the results between the three series of simulations. Of interest is that the simulations that used the mean and max input data vary significantly, even though the same P_{32} was used. This demonstrated that P_{32}, in itself, cannot be the only parameter used for characterising a given rock or structural regime. The results from the worst case demonstrated that both P_{32} and fracture size have a critical impact on the number of wedges formed along the drift. From the results obtained, it appears that the volumes passing are more influenced by fracture size than the number of fractures generated.

Figure 10 illustrates the cumulative volume plot of wedges formed around the drift. This graph can be used to assess the critical, by volume, wedge that might be encountered around the drift. This knowledge can be put in good use when developing an appropriate reinforcement strategy such as bolting pattern and rock bolt length. For example, a reinforcement rock bolting pattern can be selected to ensure that 95% of possible wedges could be secured by the standard bolt pattern. The remaining 5% of potentially unstable wedges could be stabilised by additions to the standard bolting pattern.

9   IMPACT OF THE NUMBER OF SIMULATIONS

In reviewing the form of the plots in Fig. 10, it was recognised that the worst scenario line is smooth, while the two others are step-like. This is related to the number of wedges generated. A fundamental question in this type of analysis, however, is what number of simulations is necessary to ensure that all possible wedges are captured by the models.

To investigate the impact of the number of DFN on the resulting wedges, 120 DFN models were created using the max properties defined in Section Impact of variations in
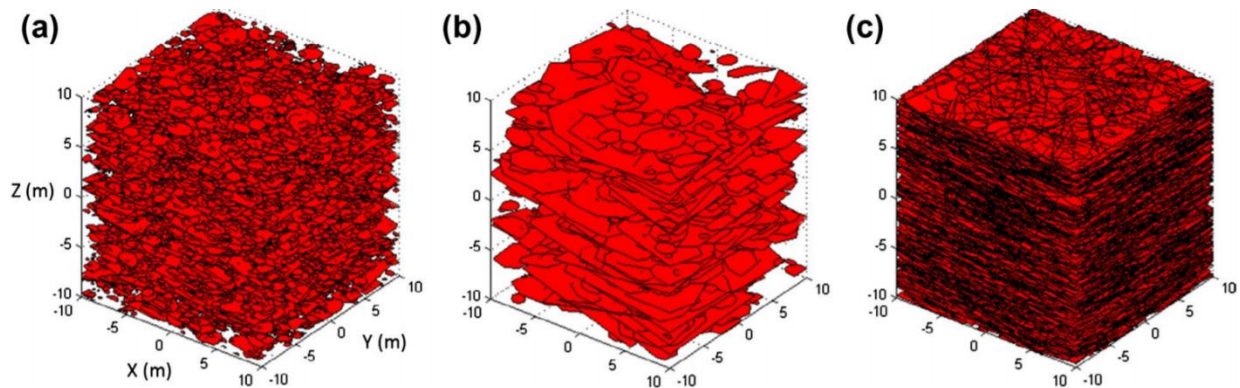

Figure 9. DFN for set 1 using *a* mean fracture representation, *b* max fracture representation, and *c* worst fracture representation using a Baecher model

Table 3. Wedge properties for the three investigated DFN inputs

	DFN input		
	Mean	Max	Worst
Number of wedges	1772	4870	2,665,348
Mean number of wedges per drift	7.8	20.3	11,105.6
Maximum volume (m³)	0.070	1.40	20.6
Volume 99th percentile (m³)	0.012	0.29	0.42
Volume 95th percentile (m³)	0.0026	0.06	0.10
Volume 90th percentile (m³)	0.0010	0.03	0.044

P32 and trace lengths. The wedges formed along the wall of a drift, within each DFN, are presented in Table 4. Figure 11 provides a graphical illustration of the information in Table 4 by presenting the volume reached after a given number of simulations. The first observation is that the total number of wedges increases with the number of simulations. The number of wedges per DFN, however, remains relatively constant. The maximum volume for a wedge along the drift was 1.37 m^3, which was reached after 60 simulations. It is recognised that a single wedge of a larger volume could be generated after a greater number of other DFN generations. For design purposes, it is the volume of wedges associated with high percentile values (for example, greater than 99th percentile) that is of interest. In this analysis, a consistent generated wedge volume was reached following 40 simulations, for high percentile values. This is the number of simulations that would appear to be adequate for this specific problem.
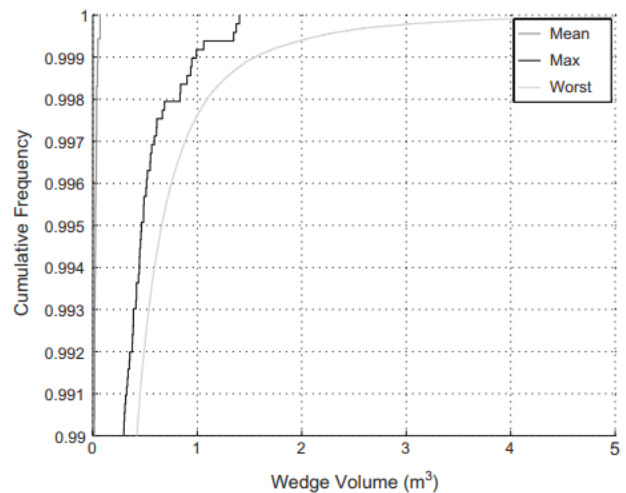

Figure 10. Wedge volume distribution along two 17-m drifts for 120 DFN models for three inputs types

Table 4. Cumulative wedge properties for various number of DFN simulations

| Number of DFN simulations	20	40	60	80	100	120
Number of wedges	346	739	1124	1506	1892	2266
Number of wedges per DFN	17.3	18.5	18.7	18.8	18.9	18.6
Maximum volume out of the realisations examined (m^3)	1.06	1.06	1.37	1.37	1.37	1.37
Volume 90th percentile (m^3)	0.0345	0.0276	0.0338	0.0345	0.0350	0.0304
Volume 95th percentile (m^3)	0.0657	0.0669	0.0785	0.0889	0.0836	0.0784
Volume 99th percentile (m^3)	0.3582	0.3780	0.3974	0.3884	0.4129	0.3881
Volume 99.5th percentile (m^3)	0.5499	0.5560	0.5568	0.5279	0.5334	0.5142
Volume 99.9th percentile (m^3)	0.8856	1.0094	1.0529	1.0259	0.9986	0.9782
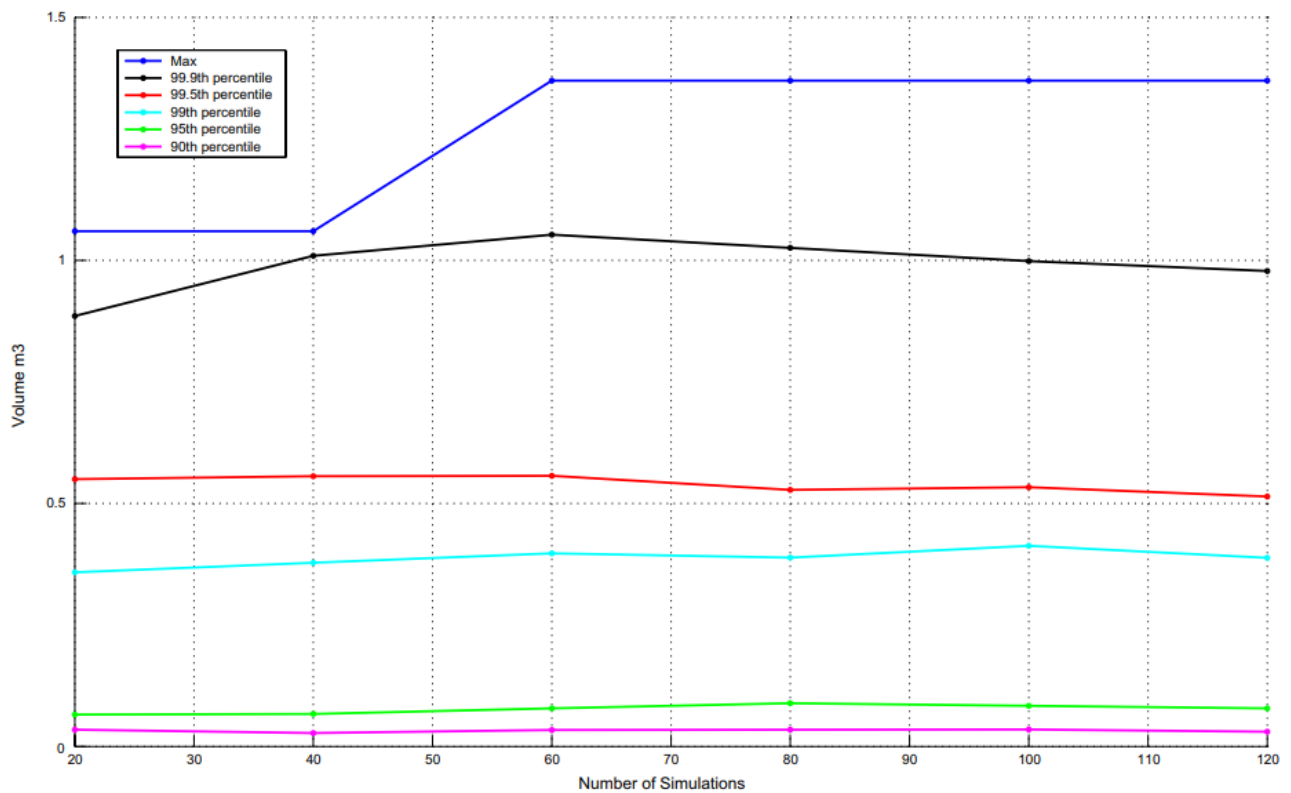
Figure 11. Wedge volume vs. the number of simulations

10 CONCLUSIONS

The use of DFN provides an additional tool in investigating the stability of underground mining drifts. This paper highlights important issues that have to be taken into consideration in order for the method to reach its full potential. The use of photogrammetry addresses some of the issues associated with data collection to ensure that the necessary input is available to generate DFN models. At the Éléonore project, photogrammetry was successfully employed to quantify the structural regime at three rock faces. The results from a photogrammetry data collection campaign were used to provide input for DFN modelling at the site. The availability of these data facilitated the calibration of these DFN models. A case study was presented on generating DFN models, and investigating their use as part of a stability investigation, for mining drifts at the Éléonore.

The primary issue in the appropriate use of DFN for practical engineering applications is the choice of a suitable model. In the presented case study, at the Éléonore site, four conceptual models, Baecher, BART, nearest neighbour and Veneziano, were used to generate the DFN models. Although all models were validated and considered statistically acceptable, the resulting generated rock masses were geometrically different. These differences can have a clear impact on the generated rock wedges and stability of underground mining drifts. In the Éléonore case study, joint termination was in intact rock, coplanarity was not observed, no clustering around major fractures were observed; thus, the simple Baecher model was deemed better suited and adequate to represent in situ conditions.

The second issue, the impact of variations in the input data, was explored by considering three different scenarios. These examples are not extreme, but can easily result as part of the assessment of the structural regime. It is demonstrated that the use of similar P32 as input does not result in similar wedge conditions.

The third issue was the number of DFN simulations needed to capture the full range of wedges. This paper demonstrated that given that DFN generation is stochastic, it is necessary to undertake multiple simulations. This is critical in gaining confidence in the results. It is understood that the maximum size wedge could arise at any given simulation, but volume obtained for high percentile values (above 99%) is reaching a plateau after a relative low number of DFN simulations for this case study.

ACKNOWLEDGEMENTS

REFERENCES

ADAM technology. 2010. 3DM analyst mine mapping suite 3D measurement, camera calibration and block adjustment software – user guide draft, Perth, ADAM technology.

Birch, J. S. 2006. Using 3DM analyst mine mapping suite for rock face characterization, in Proceedings of the laser and photogrammetric methods for rock face characterization workshop, (eds. F. Tonon and J. Kottenstette), 13–32, Minneapolis, MN, American Rock Mechanics Association.

Brady, B. H. G. and Brown, E. T. 2004. Rock mechanics for underground mining, 3rd ed., Netherlands, Kluwer Academic.

Dershowitz, W. S. and Einstein, H. H. 1988. Characterizing rock joint geometry with joint system models, Rock Mechanics and Rock Engineering, 21, (1), 21–51.

Dubois, É. and Grenon, M. 2012. Caractérisation structurale à l'aide de la photogrammétrie: mine Kikialik, Nunavik, Québec, in Proceedings of tunnels and underground spaces: sustainability and innovation, (eds. A. Rancourt), 1–8, Montreal, Tunnelling Association of Canada.

Elmo, D., Liu, Y. and Rogers, S. 2014. Principles of discrete fracture network modelling for geotechnical applications, International Discrete Fracture Engineering Conference, Vancouver: DFNE, 2014–2238.

Esmaieli, K., Hadjigeorgiou, J. and Grenon, M. 2010. Estimating representative elemental volume (REV) for rock mass properties using synthetic rock mass modeling approach, International Journal of Rock Mechanics and Mining Sciences, 47, 915–926.

Fisher, N. I., Lewis, T. and Embleton, B. J. J. 1993. Statistical analysis of spherical data, Paperback ed., Cambridge: Cambridge University Press.

Gaich, A., Pötsch, M. and Schubert, W. 2006. Basics, principles and application of 3D imaging systems with conventional and high-resolution cameras, in Proceedings of the laser and photogrammetric methods for rock face characterization workshop, (eds. F. Tonon and J. Kottenstette), 32–48, Minneapolis, MN, American Rock Mechanics Association.

Gaich, A., Pötsch, M. and Schubert, W. 2008. Computer vision for rock mass characterization in underground excavation, in Proceedings of the 42nd US Rock Mechanics Symposium, (eds. F. Tonon), 1–8, Alexandria, VA, American Rock Mechanics Association.

Golder Associates. 2008. Éléonore project site investigation report: geotechnical study for the underground mine, internal report, Montreal, Golder Associates.

Grenon, M. and Hadjigeorgiou, J. 2003a. Drift reinforcement design based on discontinuity network

modelling, International Journal of Rock Mechanics and Mining Sciences, 40, 833–845.

Grenon, M. and Hadjigeorgiou, J. 2003b. Open stope stability using 3D joint networks, Rock Mechanics and Rock Engineering, 36, (3), 183–208.

Grenon, M. and Hadjigeorgiou, J. 2008a. Fracture-SG: a fracture system generator software package, version 2.17.

Grenon, M. and Hadjigeorgiou, J. 2008b, January 7. A design methodology for rock slopes susceptible to wedge failure using fracture system modelling, Engineering Geology, 96, (1–2), 78–93, ISSN 0013-7952, http://dx.doi.org/10.1016/j.enggeo.2007.10.002.

Grenon, M. and Hadjigeorgiou, J. 2012. Applications of fracture system models (FSM) in mining and civil rock engineering design. International Journal of Mining, Reclamation and Environment, 26, (1), 55–73.

Grenon M., Lemy, F. and Hadjigeorgiou, J. 2004. Fracture system modeling based on input data from traditional mapping and image analysis, in Proceedings of EUROCK 2004 & the 53rd Geomechanics Colloquium, (eds. W. Schubert), 445–448, Salzburg.

Hadjigeorgiou, J. and Grenon, M. 2005. Design of ventilation raises in hard rock mines, in Proceedings of the 40th US Symposium on Rock Mechanics (USRMS), (ed. D. P. Yale), 1424–1430, Minneapolis, MN, American Rock Mechanics Association.

Hadjigeorgiou, J., Esmaieli, K. and Grenon, M. 2009. Stability analysis of vertical excavations in hard rock, Tunnelling and Underground Space Technology, 24, 296–308.

Hadjigeorgiou J., Lessard, J. F., Villaescusa, E. and Germain, P. 1995. An appraisal of structural mapping techniques. Second International Conference on Mechanics of Jointed and Faulted Rock, Vienna Balkema, 191–198.

Haneberg, W. C. 2008. Using close range terrestrial digital photogrammetry for 3-D rock slope modeling and discontinuity mapping in the United States, Bulletin of Engineering Geology and the Environment, 67, (4), 457–469.

Kemeny, J., Turner, K. and Norton, B. 2006. LiDAR for rock mass characterization: hardware, software, accuracy and best-practices, in Proceedings of the laser and photogrammetric methods for rock face characterization workshop, (eds. F. Tonon and J. Kottenstette), 49–61, Minneapolis, MN, American Rock Mechanics Association.

Kulatilake, P. H. S. W. and Wu, T. H. 1984. Estimation of mean trace length of discontinuities, Rock Mechanics and Rock Engineering, 17, (4), 215–232.

Lajoie, P.-L. 2013. Mise en production d'Éléonore avec ses différents défis géomécaniques, Proceedings of Québec mine, Quebec City, http://quebecmines.gouv.qc.ca/2013/programme/conferences.asp.

Mauldon, M. and Dershowitz, W. 2000. A multi-dimensional system of fracture abundance measures, Proceedings of the 112th Annual Meeting of the Geological Society of America (Summit 2000), Boulder, CO, Geological Society of America.

Pahl, P. J. 1981. Estimating the mean length of discontinuity traces, International Journal of Rock Mechanics and Mining Sciences & Geomechanics Abstracts, 18, (3), 221–228.

Priest, S. D. and Hudson, J. A. 1976. Discontinuity spacing rock, International Journal of Rock Mechanics and Mining Sciences, 13, (5), 135–148.

Rocscience. 2011. Dips v. 6.012 software information, Toronto, ON, Rocscience

Rogers, S., Elmo, D. Beddoes R. and Dershowitz W. 2009. Mine scale DFN modelling and rapid upscaling in geomechanical simulations of large open pits. Proc. Int. Conference on Large Open Pits, Santiago, Chile

Rogers, S., Elmo, D., Webb, G. and Catalan, A. 2015. Volumetric fracture intensity measurement for improved rock mass characterisation and fragmentation assessment in block caving operations, Rock Mechanics and Rock Engineering, 48, 633–649. http://dx.doi.org/10.1007/s00603-014-0592-y

Rogers, S. F., Moffitt, K. M. and Kennard, D. T. 2006. Probabilistic tunnel and slope block stability using realistic fracture network models. 41st US Rock Mechanics Symposium, Golden, ARMA/USRM 06-1052.

SRK Consulting. 2011. Structural model of the Éléonore deposit, Quebec, internal report, Perth, SRK Consulting.

Staub, I., Fredriksson, A. and Outters, N. 2002. Strategy for a rock mechanics site descriptive model development and testing of the theoretical approach, SKB report, No. R-02-02, prepared for Golder Associates AB, Stockholm.

Sturzenegger, M. and Stead, D. 2009. Close-range terrestrial digital photogrammetry and terrestrial laser scanning for discontinuity characterization on rock cuts, Engineering Geology, 106, (3–4), 163–182.

Sturzenegger, M., Stead, D., Beveridge, A., Lee, S. and van As, A. 2009. 'Long-range terrestrial digital photogrammetry for discontinuity characterization at Palabora open-pit mine', in Proceedings of the Third Canada-US Rock Mechanics Symposium and the 20th Canadian Rock Mechanics Symposium (RockEng09), (eds. M. Diederichs and G. Grasselli), 10, Toronto.

Zhang, L. and Einstein, H. H. 1998. Estimating the mean trace length of rock discontinuities, Rock Mechanics and Rock Engineering, 31, (4), 217–235.